HHS Public Access

Author manuscript

OpenNano. Author manuscript; available in PMC 2025 March 21.

Published in final edited form as:

OpenNano. 2025 March ; 22: . doi:10.1016/j.onano.2025.100235.

Osteogenic differentiation of mesenchymal stem cells in cell-laden culture of self-assembling peptide hydrogels

Faye Fouladgar[a], **Robert Powell**[a], **Vishalakshi Irukuvarjula**[a], **Akhila Joy**[b], **Xiao Li**[b], **Neda Habibi**[a,*]

[a]Department of Biomedical Engineering, University of North Texas, TX, USA

[b]Department of Material Science & Engineering, University of North Texas, TX, USA

Abstract

Mesenchymal stem cell (MSC) osteogenic differentiation requires scaffolds to support multiple stages of growth and differentiation signals. Fluorenyl-9-methoxycarbonyl diphenylalanine (Fmoc-FF) peptides self-assemble to create 3D nanofibers. Here, we cultured MSC in 2D and 3D Fmoc-FF layers to support their osteogenic differentiation. The stiffness of the hydrogels was tunable between 100 and 10,000 Pa which allows precise modulation of the cellular microenvironment. Scaffold stiffness impacted cell viability which softer scaffolds (100 Pa) favored higher viability. MSC formed spheroids in 3D hydrogel and showed spread morphology in 2D overlayers. Our results demonstrate that the Fmoc-FF 3D cultures significantly enhanced osteogenic differentiation, as evidenced by increased calcium deposition, elevated phosphatase activity, and the secretion of osteocalcin. We propose that the peptides provide integrin-binding sites that activate a cytoplasmic feedback loop essential for differentiation. These findings suggest that self-assembled Fmoc-FF peptide hydrogels, is a promising platform for bone tissue engineering applications.

Keywords

Human mesenchymal stem cells (hMSCs); Fmoc-FF peptide hydrogel; Osteogenic Differentiation

1. Introduction

Osteoporosis is a condition characterized by a decrease in bone density, which results from an imbalance between heightened bone resorption and diminished bone formation

*Corresponding author at: Nanomedicine Lab, Department of Biomedical Engineering, The University of North Texas, a Carnegie R1 Institution, Discovery Park, Office: K240E, USA. https://nanomedicine.engineering.unt.edu/ (N. Habibi).

Declaration of competing interest

The authors declare that they have no known competing financial interests or personal relationships that could have appeared to influence the work reported in this paper.

CRediT authorship contribution statement

Faye Fouladgar: Methodology, Investigation, Formal analysis, Data curation. **Robert Powell:** Methodology, Investigation. **Vishalakshi Irukuvarjula:** Methodology, Investigation. **Akhila Joy:** Methodology. **Xiao Li:** Methodology, Investigation. **Neda Habibi:** Writing – review & editing, Writing – original draft, Supervision, Project administration, Funding acquisition, Data curation, Conceptualization.

[1]. This disorder predominantly impacts older individuals and postmenopausal women [2]. Current treatment options for osteoporosis focus on anti-resorptive medications, including hormone replacement therapy (HRT), selective estrogen receptor modulators (SERMs), and antibodies targeting RANKL [3]. However, some of these treatments have been associated with side effects, including an increased risk of breast cancer and heart disease [4–6]. An optimal pharmacological approach for treating bone loss should both inhibit osteoclast activity and promote osteoblast-driven bone formation [7]. Due to the drawbacks associated with traditional treatments, researchers have explored the potential use of stem cells as an alternative approach in bone healing [8]. Mesenchymal stem cells (MSCs) are regarded as the most suitable stem cell type for osteoporosis treatment because of their widespread availability, less invasive extraction methods, and remarkable regenerative potential [9]. Mesenchymal stem cells (MSCs) have the ability to differentiate into various mesenchymal-derived tissues, including osteoblasts, adipocytes, and chondrocytes [10,11]. These cells can be readily obtained from multiple adult tissues, such as bone marrow, adipose tissue, and peripheral blood. In the context of bone repair, MSCs play a crucial role by integrating into the target site and undergoing differentiation into bone-forming cells [11]. Several key aspects will determine the cell fate of MSC to differentiate into bone: the chemical soluble factors, mechanical strains and 3D niche surrounding the cells (ECM) [12,13]. Beside the chemical factors which are established for each cell differentiation, the effect of scaffold stiffness [14] and 3D culture [15] in determining cell fate of MSC is still not well understood [16,17]. It has been indicated that in vitro mechanical stretch can modulate the balance of self-renewal and differentiation dependent on the cell types [18,19].

While conventional two-dimensional (2D) cell culture on treated petri dish or flask remains commonly practiced, studies have demonstrated that transitioning stem cells from their native 3D environment leads to unnatural cell distribution within ECM, altered growth kinetics, and significantly impacts their differentiation potential. In this regard, culturing MSCs in 2D environments has been associated with a reduction in multipotency and early onset of cellular senescence. To overcome these challenges, various 3D culture techniques have been explored, including the use of scaffold-free spheroid cultivation. Conversely, reports on the impact of 3D culture on cell viability is often contradictory. While some studies reported an increase in viability and proliferation compared to the respective 2D controls [20], others observed opposite effects [21]. Moreover, these approaches typically target enhancing biological activity at a single stage of tissue development, such as promoting cell attachment. Supporting the various stages required to create functional engineered tissue necessitates multiple biological components and signals that must be precisely coordinated in both spatial and temporal aspects [20].

To address these needs, here, we focused on using peptide hydrogelators based on Fmoc-Phenylalanine-Phenylalanine (Fmoc-FF) to culture MSC in 3D and promote osteogenic differentiation. Supramolecular hydrogelators made from short peptides offer several benefits over traditional polymeric hydrogels [22]: (i) they have adjustable stiffness to regulate cell fate and unique self-healing properties (ii) they are generally more biocompatible and biodegradable due to the non-covalent interactions between molecules and (iii) they more closely resemble the extracellular matrix (ECM) since the self-assembled nanostructures typically range from 5 to 300 nm [23] (iv) they have shown to promote

differentiation in various cells including dermal fibroblast cells [24]. Here, we use 3D peptide hydrogel culture to accelerate osteogenic differentiation of MSC. To this aim, we prepared various stiffness of Fmoc-FF gels and studied their mechanical properties and its effect on cell viability [25]. MSC were seeded in 2D and 3D Fmoc-FF hydrogels and osteogenic differentiation were studied. This study explores the potential impact of stiffness on cell viability and osteogenic differentiation in 3D cultures, highlighting the role of peptide hydrogelators in maintaining cell viability and promoting osteogenic differentiation, which may offer valuable insights for bone tissue regeneration.

2. Materials and methods

2.1. Materials

Mesenchymal Stem Cell derived from Bone marrow was acquired from Fisher Scientific, USA (Catalog No.SCC034), as a cryopreserved vial and stored in a liquid nitrogen tank prior to use. The cells were maintained in growth medium Minimum Essential Medium Eagle - Alpha Modification (MEM α catalog no 12–561–056) which was supplemented with certified Fetal Bovine Serum (FBS; catalog no 16,000,069) and antibiotics, all were purchased from ThermoFisher Scientific. Trypsin-EDTA and Fmoc-Phenylalanyl-phenylalanine (Phe-Phe catalog no J60043.03) were also obtained from ThermoFisher Scientific. Hexafluoroisopropanol (HFP/1,1,1,3,3,3-Hexafluoro-2-propano catalog no 105,228) was obtained from Millipore Sigma. Alexa Fluor 488 Phalloidin (catalog no A12379), DAPI (catalog no D1306), Alizarin Red assay kit (catalog no A12379) Alkaline Phosphatase assay kit (catalog no 637,944), Osteocalcin immunostaining (catalog no OSTCLN-FITC), ascorbate-2 phosphate (ThermoFisher Scientific, catalog number A25215 G), 10^{-8} M dexamethasone (A17590.14, ThermoFisher Scientific), and β-glycerophosphate (J62121.AD ThermoFisher Scientific), MTT (catalog no V13154), LIVE-Dead (catalog no L32250) were also obtained.

2.2. Synthesis of Fmoc-FF hydrogel

Peptide hydrogels were developed using Fmoc-FF obtained from Bachem, Germany, with a purity of 99 %. Peptides were dissolved in HFP (Hexafluoroisopropanol, 99 %) or DMSO with a stock concentration of 100 mg/ml, and subsequently diluted to final concentrations of 1–10 % using sterilized water for hydrogel preparation. The solution was maintained in a sterilized environment at 20 °C.

2.3. Scanning electron microscopy

Fmoc-FF hydrogels deposited on silicone substrates were imaged using scanning electron microscopy (SEM) to analyze surface morphology and structural features. SEM imaging was performed at an accelerating voltage of 5–10 kV, allowing for high-resolution visualization of the Fmoc-FF hydrogel structures and their interaction with the silicone surface.

2.4. Mechanical properties Fmoc-FF hydrogel

To evaluate the physical properties of the peptide hydrogels, amplitude sweeps, and viscosity tests were conducted using a parallel plate rheometer (Anton Paar MCR92). These tests

provided insights into the mechanical behavior and flow properties of the hydrogels. Peptide hydrogels 1–10 % in DMSO and HFP were tested with a 25 mm parallel plate (PP-25). Amplitude sweeps, comprising 21 data points, were performed at shear strains ranging from 0.01 % to 100 %, with a constant angular frequency of 10 rad/s and a force-controlled profile set to 0.1 N. This force-controlled approach ensured consistency between samples despite minor height variations, rather than relying on a fixed gap setting.

2.5. Cell-laden of MSC in Fmoc-FF hydrogels

Culturing human mesenchymal stem cells (MSC) derived from bone marrow involved the use of α-MEM medium supplemented with 1 % l-Glutamine, 16 % Fetal Bovine Albumin, and 1 % antibiotic solution. Upon achieving a confluent cell density, trypsinization with Trypsin-EDTA was performed, and cells were resuspended in α-MEM medium. In surface-coated hydrogel, peptide hydrogel is coated on the petri dish, and cells are seeded on top (2D cell culture). For the surface coated, the self-assembled Fmoc-FF/HFIP diluted in PBS was coated on microplate wells allowing them to dry. The cells were then seeded on the coated dish and wells. In the “Overlay Hydrogel” approach, peptide hydrogel is coated on top of the seeded cells (2D cell culture). In this approach, cells were seeded on the plates. 100 μl of Fmoc-FF were dispersed in growth medium and the hydrogel were seeded on top of the cells. In the “Infused Hydrogel”, cells are infused within the peptide hydrogel (3D cell culture). For the infused hydrogel (3D), 100 μl of Fmoc-FF was introduced into the microplate, and growth medium containing MSC cells was added to the wells. The mixture was carefully pipetted to ensure the homogeneity of the hydrogels. The infused hydrogel was kept in cell inserts and the growth medium were changed every 2 days. As a control, cells were also seeded on 2D petri dishes without hydrogels (Fig. 1).

2.6. Viability test with alamar blue reduction

MSC were seeded in the gels. After 7 days, the medium were removed, each well was washed with PBS, and of growth medium was added to each well along with 100 μL of alamarBlue HS reagent. Plates were incubated for 1–4 h at 37 °C. After incubation with the reagent, absorbance of each well was read with a microplate reader at 570 nm, along with 600 nm as a reference wavelength. Absorbance readings were used to calculate the percentage reduction of the alamarBlue reagent using the equation below.

$$\%\ Reduction\ of\ alamarBlue\ Reagent = \frac{(E_{oxi}600 \times A_{570}) - (E_{oxi}570 \times A_{600})}{(E_{red}570 \times C_{600}) - (E_{red}600 \times C_{570})} \times 100$$

where E is the molar extinction coefficient of the oxidized or reduced alamarBlue Reagent, A is the absorbance of the test wells, and C is the absorbance of the negative control wells with only cell culture medium and alamarBlue Reagent at 570 nm and 600 nm.

2.7. Cell viability with live-dead assay

Cell viability was evaluated using a LIVE/DEAD assay with the LIVE/DEAD Viability/Cytotoxicity Kit, following the protocol provided by the manufacturer. In brief, cells were incubated with a solution containing calcein-AM and ethidium homodimer-1 for 30 min at room temperature. After incubation, the cell/gel constructs were centrifuged, rinsed, and

prepared for analysis. Fluorescence microscopy was employed to visualize the cells, where viable cells exhibited green fluorescence due to calcein-AM, and non-viable cells displayed red fluorescence from ethidium homodimer-1. The proportion of live and dead cells was quantified using ImageJ software, and all experiments were performed in triplicate to ensure reproducibility and reliability of the data.

2.8. Staining cytoplasm with Phalloidin and nucleus with DAPI

Cells were fixed with 4 % paraformaldehyde, permeabilized with 0.1 % Triton X-100, and blocked with 1 % BSA in PBS for 1 h. F-actin cytoskeleton was visualized using Phalloidin. All steps were conducted following the manufacturer's instructions, and the experiments were performed in triplicate for accuracy.

2.9. In-vitro bone differentiation of MSC in Fmoc-FF hydrogel

For osteogenic differentiation, the cells underwent osteogenic induction in a specialized medium, termed osteogenic induction medium (OIM). This medium consisted of α-MEM-LG supplemented with 10 % FBS, ascorbate-2 phosphate (Thermofisher), 10^{-8} M dexamethasone (Thermofisher), and 1×10^{-2} mβ-glycerophosphate (Thermofisher). Growth medium was replaced with OIM after 3 days of seeding.

2.10. Alizarin assay

For the Alizarin assay, the growth medium was aspirated, and cells were rinsed with PBS to remove any residual medium. Subsequently, cell fixation was achieved by treating the cells with a 4 % paraformaldehyde solution. Alizarin Red, a dye known for its strong affinity for calcium ions, was then employed to stain the fixed cells. The stained cells underwent incubation with the Alizarin reagent, followed by exposure to acetic acid. This acid treatment facilitated the extraction of the bound dye from the stained cells. The quantification of the extracted dye was done by measuring the absorbance at 590 nm wavelength. This step provides a quantitative assessment of the calcium deposits within the cells, and the osteogenic activity.

2.11. Alkaline phosphatase assay

Alkaline phosphatase plays a crucial role in mineralization processes, particularly in the context of osteogenesis and bone formation. Therefore, alkaline phosphatase staining is often employed as an indicator of early osteogenic differentiation in cell cultures. On day 14, the media were removed, and cells were fixed with a fixative. After discarding the fixative, the cells were rinsed with PBS. A sufficient amount of the ALP stain solution was prepared following the protocol provided by the manufacturer and then incubated in the dark. The number of colonies expressing ALP (red) versus the undifferentiated colonies (colorless) was then counted.

2.12. Osteocalcin assay

Cells were plated at a density of 5×10^4 cells per well and cultured at 37 °C in a humidified atmosphere with 5 % CO_2. Following incubation, the cells were fixed using 400 μL of 4 % paraformaldehyde (pH 7.4) for 10 mins at 37 °C. The fixative was subsequently removed,

and the cells were rinsed three times with 1 mL of PBS. To permeabilize the cells, 500 μL of 0.1 % Triton X-100 in PBS was added, and the samples were incubated at room temperature for 10–15 mins. For immunostaining, a FITC-labeled osteocalcin polyclonal antibody was diluted 1:250 in PBS, and the samples were incubated with the antibody for 1–2 h at room temperature or overnight at 4 °C in the dark. The samples were then examined under a fluorescence microscope using a green channel with an excitation wavelength near 490 nm and an emission wavelength around 520 nm to visualize osteocalcin expression.

2.13. Statistical analysis

Statistical analysis was performed in Excel XL toolbox NG using one-way ANOVA and *t*-test. Each experiment was repeated with 3 technical replicates per experiment. P values <0.001 (***), 0.01 (**), and 0.05 (*) are considered significant.

3. Results and discussion

3.1. Stiffness of Fmoc-FF based on solvent and concentration

Controlling the fate of mesenchymal stem cells (MSCs) requires optimizing the scaffold stiffness. In this study, we prepared Fmoc-FF hydrogels using solvents HFIP and DMSO at varying concentrations (1–10 %) to regulate the stiffness and examine its influence on MSC fate. By adjusting the Fmoc-FF concentration, we found that concentrations between 2 % and 10 % (w/v) (for both DMSO and HFIP-based hydrogels) resulted in stable 3D structures that maintained their integrity over multiple days. In contrast, the 1 % Fmoc-FF hydrogel exhibited liquid-like properties, while concentrations from 2 % to 10 % displayed viscoelastic having both solid-like and liquid-like characteristics.

Using parallel plate rheology, we assessed the storage modulus (G') within the linear viscoelastic region (LVR) of the hydrogels after 24 h of gelation (Fig. 2). The storage modulus increased with Fmoc-FF concentration, ranging from approximately 100 Pa at 1–2 % to 1000 Pa at 5 %, and reaching 10,000 Pa at 10 % Fmoc-FF. HFIP-based hydrogels exhibited slightly higher storage modulus values compared to their DMSO counterparts, indicating a solvent-dependent effect on hydrogel stiffness.

Rheological studies reveal that while Fmoc-FF hydrogels exhibit reliable stiffness, however they are sensitive to shear stress. Application of shear stress to these gels disrupts their structure integrity, leading to a loss of water from the gels. Although the ability to fabricate hydrogels with varying stiffness is crucial for regenerative medicine and 3D cell culture, it is also essential for these materials to withstand extrusion pressures suitable for bioprinting cell-laden hydrogels. This challenge could be addressed by developing hybrid hydrogels, such as alginate/Fmoc-FF composites, which offer enhanced mechanical stability and improved printability under conditions compatible with bioprinting. In the absence of shear stress, the Fmoc-FF hydrogels maintained their structural integrity for several days. To gain further insights into the self-assembly of Fmoc-FF peptides over time and in different solvents, we used scanning electron microscopy (SEM) to image Fmoc-FF in HFIP and DMSO at 1 h and 24 h after gel formation (Fig. 3). The SEM images reveal that the Fmoc-FF gel in HFIP quickly develops a dense fiber network within 1 hour, which becomes

more consolidated by 24 h. In contrast, the DMSO-based gel does not exhibit a fiber network at 1 hour but does form a gel by 24 h. However, the fiber network in the DMSO gel is slightly less compact compared to the HFIP gel, suggesting that solvent choice influences self-assembly time, the density, and structure of the fiber network. The SEM images also confirmed the rheology properties as DMSO gels were less compact compared to HFP gels. Fmoc-FF is best dissolved in HFIP and therefore the self-assembly process is completed making dense fibers.

Material stiffness is commonly quantified using the elastic modulus (Young's modulus) for solid materials and the storage modulus for viscoelastic materials. To effectively guide stem cell differentiation toward specific tissue lineages [26], the stiffness of scaffolds should ideally mimic the mechanical properties of the native tissue [27]. For example, substrates with stiffness values similar to the elastic modulus of brain tissue (0.1–1 kPa), pancreas (1.2 kPa), cartilage (3 kPa)) [28,29], muscle (8–17 kPa), and bone tissue (25–40 kPa) [30,31] have been shown to direct mesenchymal stem cells (MSCs) to differentiate into neurocytes, beta cells, chondrocytes, myoblasts, and osteoblasts, respectively. These mechanical cues play a critical role in stem cell fate determination and tissue engineering applications [32]. Preliminary studied on stiffness indicates that Fmoc-FF provide adjustable stiffness that can accommodate bone differentiation. However, it's important to understand how stiffness is impacting the viability, proliferation and differentiation.

3.2. Viability of MSC encapsulate in Fmoc-FF hydrogel

We evaluated the effect of hydrogel stiffness on mesenchymal stem cell (MSC) viability by encapsulating cells within Fmoc-FF hydrogels and assessing viability using the alamar blue assay (Fig. 4A). Hydrogels formulated with HFIP showed higher cell viability compared to those prepared with DMSO. Specifically, MSCs suspended in 1 % Fmoc-FF/HFIP hydrogels maintained 80 % viability, which increased to 87 % when the concentration was raised to 2 % Fmoc-FF. Conversely, further increases in gel concentration to 5 % and 10 % led to a significant reduction in viability, decreasing to 74 % and 54 %, respectively. These findings indicate that an optimum hydrogel stiffness enhances cell survival, however, excessive stiffness exerts mechanical stress detrimental to cell viability. This observation was confirmed by LIVE-DEAD fluorescence assays, which confirmed a majority of viable cells, with relatively few dead cells in Fmoc-FF HFIP gels. DMSO-based gels led to a higher proportion of dead cells (Fig. 4B).

Studies have shown that the impact of 3D culturing on cell viability and proliferation relies on both the cell type and the specific cultivation technique employed. Some studies have reported enhanced viability and proliferation compared to 2D controls, while others have noted reduced cell viability in 3D cultures [33]. These differences are likely due, at least in part, to the distinct characteristics of various 3D cell culture methods. Given that osteoporosis and aging tend to impair the viability and proliferation of MSCs, it is crucial to evaluate the effects of 3D cell culture technology on these parameters. Such assessments are essential for the development of effective therapeutic strategies. Briefly, spheroid cell cultures are often linked to reduced cellular proliferation and viability, whereas 3D hydrogels tend to exhibit performance that is comparable to or superior than that of 2D

cultures. In contrast to studies reporting that spheroid culture negatively affects proliferation and viability in other cell types, such as cancer cells, the impact of spheroid cultivation on MSCs remains controversial.

Some studies have indicated that MSCs within spheroids experience enhanced cell viability [20]and proliferation. However, other research has found either no change or even a decrease in cell proliferation. These varying results may be due to insufficient nutrient and oxygen distribution, as well as hindered waste removal within the core, particularly when spheroids exceed a critical size [34].

Similar to the mixed findings regarding the influence of spheroid cultures on cell viability and proliferation, the effects of 3D cultures of MSCs within scaffolds and hydrogels are multifaceted. Some 3D scaffolds—such as gelatin, PLGA, and chitosan—appear to have little to no impact on MSC viability and proliferation, other materials have been shown to alter these properties. For instance, collagen demonstrates variable effects that depend on both its method of preparation and the MSC source. Lo and collaborators found no notable alterations in the viability or proliferation of human MSCs embedded in collagen matrices. In contrast, studies have demonstrated that rat bone marrow-derived MSCs (BM-MSCs) exhibit enhanced proliferation when cultured within the same type of scaffold. Based on our findings, 2 % Fmoc-FF in HFIP with a storage modulus of 100 Pa was identified as the optimal condition for maintaining MSC viability and was used in further experiments.

3.3. Morphology and viability of MSC in 2D and 3D Fmoc-FF hydrogel

We employed various techniques to seed MSCs within the hydrogel. In the surface-coated hydrogel approach, the peptide hydrogel was coated onto the petri dish, and cells were seeded on top, mimicking a 2D cell culture. For the overlay hydrogel technique, the peptide hydrogel was layered over previously seeded cells, also representing a 2D culture condition. In the infused hydrogel method, cells were directly infused into the peptide hydrogel, creating a 3D culture environment. Observing the morphology of MSCs seeded in Fmoc-FF hydrogel using cytoplasm actin staining revealed distinct characteristics: in all 2D conditions, MSCs exhibited a spread actin morphology, whereas MSCs in the 3D infused hydrogel displayed a thinner, rounded morphology (Fig. 4C).

Matrix stiffness has been shown to influence cell morphology across various cell types, especially in 2D culture models. This effect may be due to substrate stiffness-induced alterations in integrin binding, adhesion strength, and cellular stiffness or contractility [28,30,35,36]. The morphology of a cell is influenced by both the internal organization of its cytoskeleton and its external connections with the extracellular matrix (ECM) and neighboring cells. Cell shape plays a critical role in guiding the differentiation of mesenchymal stem cells (MSCs) [37].

Previously, it was shown that MSCs with a rounded morphology on smaller areas primarily underwent adipogenesis, [38] whereas those on larger islands with a spread morphology favored osteogenesis [39,40]. Briefly, we suggest that in 2D scaffolds, substrate stiffness is generally found to affect cellular morphology, while in 3D hydrogels MSCs retain a spherical morphology irrespective of the hydrogel stiffness.

Specifically, spread-out cellular morphology is advantageous for scaffolds engineered to emulate tissues such as skin, bone, and muscle, where robust cell adhesion, extracellular matrix (ECM) synthesis, and cellular migration are critical for tissue regeneration and integration [41]. Our study illustrates that a 2D peptide coating directs cells toward a stretched and aligned phenotype more prominently than control conditions, potentially enhancing their differentiation capacity through structural and biomechanical cues. Conversely, spherical cell morphology proves beneficial in scaffolds designed to promote cell-cell interactions, such as those utilized for cartilage repair or organoid development, where three-dimensional cellular aggregates enhance tissue formation and functional differentiation. The spherical cellular arrangement observed within Fmoc-FF hydrogels highlights the material's capacity to establish a microenvironment that preserves cellular integrity and minimizes excessive adhesion, thereby fostering conditions optimal for controlled tissue morphogenesis.

Studying the viability of MSC with Calcein AM (LIVE-DEAD) staining showed that most cells are alive and only few dead cells were observable (Fig. 5). The 3D infused gel showed the highest number of live cell and least dead cells with respect to control.

3.4. Osteogenic differentiation of MSC in Fmoc-FF hydrogel

During osteogenic differentiation of MSCs, ARS staining was used to assess the presence of calcium deposits. Cells cultured in OIM showed an enhanced accumulation of calcium-rich deposits compared to those cultured in GM. Cells cultured with OIM and without peptide gels were used as controls. Surface-coated, overlay, and infused hydrogel conditions were assessed. Cells embedded within the hydrogel were placed in the upper well of a 12-well transwell plate and induced in OIM for up to 14 days. Initially, cells were cultured in growth medium (GM) for 3 days before transitioning to OIM.

MSCs cultured in 3D infused hydrogels demonstrated the highest levels of calcium deposition, indicating a strong osteogenic differentiation response. The 2D overlay hydrogel condition also showed enhanced calcium accumulation compared to the control (Fig. 6). These results, suggest that both 3D infused and 2D overlay hydrogels support osteogenic differentiation more effectively than control cultures. This may suggest that both the peptide hydrogel stiffness in 2D layers and the 3D environment are impacting calcium deposition.

During osteogenic differentiation, alkaline phosphatase (ALP) activity serves as an indicator of MSC progression toward osteoblasts. We evaluated ALP activity in MSCs cultured within peptide hydrogels, where cells with increased ALP activity were stained red (Fig. 7). As shown in Fig. 7, 3D culture of MSCs in peptide hydrogels exhibited significantly elevated ALP activity, suggesting enhanced differentiation. 2D culture of MSC with peptide hydrogel did not induce ALP activity and the control cells also showed low ALP activity. This result may suggest that the 3D environment is having an impact on increased ALP activity.

We also assessed osteocalcin expression as a biomarker for osteogenic differentiation in MSCs (Fig. 8). Osteocalcin, a late-stage marker, typically appears within 14–21 days of differentiation. MSCs cultured in 3D peptide hydrogels exhibited the highest osteocalcin expression compared to the control and 2D layers. Overall, osteogenic markers were

significantly elevated in the presence of the peptide, with 3D cultures further enhancing osteogenic differentiation relative to 2D cultures. We suggest that peptide provides integrin binding site to MSC and initiates the cytoplasm feedback loop to proceed with differentiation.

There is an increasing interest in investigating on how stem cells perceive and respond to particular stiffness levels in 2D and 2D environments [42], how these mechanical cues are translated into intracellular signaling pathways [43], and ultimately determine stem cell fate. While the effect of 3D culture on MSC viability remains debated, most studies suggest that 3D cell culture systems promote enhanced osteogenic differentiation compared to conventional 2D cultures [44,45]. It has been shown that spheroids of rat BMMSCs exhibits greater osteogenic potential compared to 2D cultures [46]. This is indicated by elevated Osterix expression, enhanced ALP activity, and increased levels of mineralization in vitro. Recent experiments in 2D models suggest that the mechanotransduction mechanism in stem cells likely involves an integrin-cytoskeletal feedback loop [47], linking mechanical and biochemical signals within the cellular signaling pathways to influence cell fate [48]. In 3D environments, which more closely mimic physiological conditions, distinct mechanisms of stiffness-based mechanotransduction may also play a role.

Nonetheless, the differentiation of encapsulated MSCs remains largely influenced by the stiffness of the hydrogel [37,49], with stiffer matrices promoting osteogenesis and softer ones favoring adipogenesis. Osteogenic differentiation on rigid substrates has been shown to require integrin binding, while the lack of integrin binding on soft matrices appears to have minimal impact on MSC differentiation toward adipogenic or neurogenic pathways [40,50]. In both 2D and 3D cultures, studies have shown that as matrix stiffness increases, the binding of integrins to the matrix follows a bell-shaped distribution. The stiffness of the hydrogel that promotes maximum integrin binding also appears to be the most conducive for osteogenic differentiation [51,52].

4. Conclusion

Our study demonstrated that mesenchymal stem cells (MSCs) seeded in a 3D Fmoc-FF peptide hydrogel show a significant increase in osteogenic differentiation. Interestingly, even 2D layers of the peptide hydrogel promoted osteogenic differentiation indicated by calcium deposition, suggesting that hydrogel stiffness also plays a role in this process. The Fmoc-FF hydrogel allows for controlled stiffness ranging from 10 to 10,000 Pa, which supports MSC differentiation. Scaffold stiffness impacted cell viability which softer scaffolds (100 Pa) favored higher viability compared to stiffer scaffolds (10 kPa). The optimal stiffness for preserving MSC viability was 100 Pa, corresponding to a 2 % Fmoc-FF in HFIP solution. We propose that the peptides provide integrin-binding sites that activate a cytoplasmic feedback loop essential for differentiation. Therefore, Fmoc-FF hydrogel presents itself as a suitable scaffold for MSC-based tissue engineering, with potential applications in cell therapies and regenerative medicine.

Acknowledgment

This work was supported by the National Institute of General Medical Science (NIGMS) of the National Institutes of Health under award number R16GM150848.

References

[1]. Sozen T, Ozisik L, Calik Basaran N, An overview and management of osteoporosis, Eur. J. Rheumatol. 4 (1) (2017) 46–56, 10.5152/eurjrheum.2016.048. [PubMed: 28293453]

[2]. Black DM, Rosen CJ, Postmenopausal osteoporosis, New England J. Med. 374 (3) (2016) 254–262, 10.1056/NEJMcp1513724. [PubMed: 26789873]

[3]. Jimi E, Hirata S, Osawa K, Terashita M, Kitamura C, Fukushima H, The current and future therapies of bone regeneration to repair bone defects, Int. J. Dent. 2012 (2012) 1–7, 10.1155/2012/148261.

[4]. Salari Sharif P, Abdollahi M, Larijani B, Current, new and future treatments of osteoporosis, Rheumatol. Int. 31 (3) (2011) 289–300, 10.1007/s00296-010-1586-z. [PubMed: 20676643]

[5]. Rizzoli R, et al. , Management of osteoporosis in the elderly, Curr. Med. Res. Opin. 25 (10) (2009) 2373–2387, 10.1185/03007990903169262. [PubMed: 19650751]

[6]. Isaksson E, et al. , Expression of estrogen receptors (α, β) and insulin-like growth factor-I in breast tissue from surgically postmenopausal cynomolgus macaques after long-term treatment with HRT and tamoxifen, The Breast 11 (4) (2002) 295–300, 10.1054/brst.2002.0422. [PubMed: 14965685]

[7]. Demontiero O, Vidal C, Duque G, Aging and bone loss: new insights for the clinician, Ther. Adv. Musculoskelet. Dis. 4 (2) (2012) 61–76, 10.1177/1759720X11430858. [PubMed: 22870496]

[8]. Macías I, Alcorta-Sevillano N, Rodríguez CI, Infante A, Osteoporosis and the potential of cell-based therapeutic strategies, Int. J. Mol. Sci. 21 (5) (2020) 1653, 10.3390/ijms21051653. [PubMed: 32121265]

[9]. Andrzejewska A, Lukomska B, Janowski M, Concise review: mesenchymal stem cells: from roots to boost, Stem Cells 37 (7) (2019) 855–864, 10.1002/stem.3016. [PubMed: 30977255]

[10]. Gilkeson GS, Safety and efficacy of mesenchymal stromal cells and other cellular therapeutics in rheumatic diseases in 2022: a review of what we know so far, Arthritis Rheumat. 74 (5) (2022) 752–765, 10.1002/art.42081.

[11]. Phetfong J, et al. , Osteoporosis: the current status of mesenchymal stem cell-based therapy, Cell Mol. Biol. Lett. 21 (1) (2016) 12, 10.1186/s11658-016-0013-1. [PubMed: 28536615]

[12]. Pino AM, Rosen CJ, Rodríguez JP, In osteoporosis, differentiation of mesenchymal stem cells (MSCs) improves bone marrow adipogenesis, Biol. Res. 45 (3) (2012) 279–287, 10.4067/S0716-97602012000300009. [PubMed: 23283437]

[13]. Aghebati-Maleki L, et al. , Prospect of mesenchymal stem cells in therapy of osteoporosis: a review, J. Cell Physiol. 234 (6) (2019) 8570–8578, 10.1002/jcp.27833. [PubMed: 30488448]

[14]. Mousavi SJ, Hamdy Doweidar M, Role of mechanical cues in cell differentiation and proliferation: a 3D numerical model, PLoS. One 10 (5) (2015) e0124529, 10.1371/journal.pone.0124529. [PubMed: 25933372]

[15]. Huang C, Dai J, Zhang XA, Environmental physical cues determine the lineage specification of mesenchymal stem cells, Biochimica et Biophysica Acta (BBA) - Gen. Subj. 1850 (6) (2015) 1261–1266, 10.1016/j.bbagen.2015.02.011.

[16]. Hao J, et al. , Mechanobiology of mesenchymal stem cells: perspective into mechanical induction of MSC fate, Acta Biomater. 20 (2015) 1–9, 10.1016/j.actbio.2015.04.008. [PubMed: 25871537]

[17]. Chen T, Yang T, Zhang W, Shao J, The therapeutic potential of mesenchymal stem cells in treating osteoporosis, Biol. Res. 54 (1) (2021) 42, 10.1186/s40659-021-00366-y. [PubMed: 34930472]

[18]. Steward AJ, Kelly DJ, Mechanical regulation of mesenchymal stem cell differentiation, J. Anat. 227 (6) (2015) 717–731, 10.1111/joa.12243. [PubMed: 25382217]

[19]. Ghazanfari S, Tafazzoli-Shadpour M, Shokrgozar MA, Effects of cyclic stretch on proliferation of mesenchymal stem cells and their differentiation to smooth muscle cells, Biochem. Biophys. Res. Commun. 388 (3) (2009) 601–605, 10.1016/j.bbrc.2009.08.072. [PubMed: 19695226]

[20]. Spreda M, Hauptmann N, Lehner V, Biehl C, Liefeith K, Lips KS, Porous 3D scaffolds enhance MSC vitality and reduce osteoclast activity, Molecules. 26 (20) (2021) 6258, 10.3390/molecules26206258. [PubMed: 34684837]

[21]. Kusuma GD, et al. , Effect of 2D and 3D culture microenvironments on mesenchymal stem cell-derived extracellular vesicles potencies, Front. Cell Dev. Biol. 10 (2022), 10.3389/fcell.2022.819726.

[22]. Wang Y, et al. , Self-assembled peptide-based hydrogels as scaffolds for proliferation and multi-differentiation of mesenchymal stem cells, Macromol. Biosci. 17 (4) (2017), 10.1002/mabi.201600192.

[23]. Fouladgar F, et al. , Mesenchymal stem cells aligned and stretched in self-assembling peptide hydrogels, Heliyon. 10 (1) (2024) e23953, 10.1016/j.heliyon.2023.e23953. [PubMed: 38234902]

[24]. Zhou M, et al. , Self-assembled peptide-based hydrogels as scaffolds for anchorage-dependent cells, Biomaterials 30 (13) (2009) 2523–2530, 10.1016/j.biomaterials.2009.01.010. [PubMed: 19201459]

[25]. Kumar P, Nagarajan A, Uchil PD, Analysis of cell viability by the MTT assay, Cold. Spring. Harb. Protoc. 2018 (6) (2018) pdb.prot095505, 10.1101/pdb.prot095505.

[26]. Lv H, et al. , Mechanism of regulation of stem cell differentiation by matrix stiffness, Stem Cell Res. Ther. 6 (1) (2015) 103, 10.1186/s13287-015-0083-4. [PubMed: 26012510]

[27]. Wells RG, The role of matrix stiffness in regulating cell behavior, Hepatology 47 (4) (2008) 1394–1400, 10.1002/hep.22193. [PubMed: 18307210]

[28]. Solon J, Levental I, Sengupta K, Georges PC, Janmey PA, Fibroblast adaptation and stiffness matching to soft elastic substrates, Biophys. J. 93 (12) (2007) 4453–4461, 10.1529/biophysj.106.101386. [PubMed: 18045965]

[29]. Islam A, Mbimba T, Younesi M, Akkus O, Effects of substrate stiffness on the tenoinduction of human mesenchymal stem cells, Acta Biomater. 58 (2017) 244–253, 10.1016/j.actbio.2017.05.058. [PubMed: 28602855]

[30]. Park JS, et al. , The effect of matrix stiffness on the differentiation of mesenchymal stem cells in response to TGF-β, Biomaterials 32 (16) (2011) 3921–3930, 10.1016/j.biomaterials.2011.02.019. [PubMed: 21397942]

[31]. Wan W, et al. , Synergistic effect of matrix stiffness and inflammatory factors on osteogenic differentiation of MSC, Biophys. J. 117 (1) (2019) 129–142, 10.1016/j.bpj.2019.05.019. [PubMed: 31178039]

[32]. Chen J, et al. , Cell mechanics, structure, and function are regulated by the stiffness of the three-dimensional microenvironment, Biophys. J. 103 (6) (2012) 1188–1197, 10.1016/j.bpj.2012.07.054. [PubMed: 22995491]

[33]. Cesarz Z, Tamama K, Spheroid culture of mesenchymal stem cells, Stem Cells Int. 2016 (1) (2016), 10.1155/2016/9176357.

[34]. Jauković A, et al. , Specificity of 3D MSC spheroids microenvironment: impact on MSC behavior and properties, Stem Cell Rev. Rep. 16 (5) (2020) 853–875, 10.1007/s12015-020-10006-9. [PubMed: 32681232]

[35]. Park CK, Xu ZZ, Liu T, Lü N, Serhan CN, Ji RR, Resolvin D2 is a potent endogenous inhibitor for transient receptor potential subtype V1/A1, inflammatory pain, and spinal cord synaptic plasticity in mice: distinct roles of Resolvin D1, D2, and E1, J. Neurosci. 31 (50) (2011) 18433–18438, 10.1523/JNEUROSCI.4192-11.2011. [PubMed: 22171045]

[36]. Chowdhury F, et al. , Material properties of the cell dictate stress-induced spreading and differentiation in embryonic stem cells, Nat. Mater. 9 (1) (2010) 82–88, 10.1038/nmat2563. [PubMed: 19838182]

[37]. McBeath R, Pirone DM, Nelson CM, Bhadriraju K, Chen CS, Cell shape, cytoskeletal tension, and RhoA regulate stem Cell lineage commitment, Dev. Cell 6 (4) (2004) 483–495, 10.1016/S1534-5807(04)00075-9. [PubMed: 15068789]

[38]. Sefcik LS, et al. , Collagen nanofibres are a biomimetic substrate for the serum-free osteogenic differentiation of human adipose stem cells, J. Tissue Eng. Regen. Med. 2 (4) (2008) 210–220, 10.1002/term.85.

[39]. Zhao X, Huebsch N, Mooney DJ, Suo Z, Stress-relaxation behavior in gels with ionic and covalent crosslinks, J. Appl. Phys. 107 (6) (2010), 10.1063/1.3343265.

[40]. Parekh AB, Decoding cytosolic Ca2+ oscillations, Trends. Biochem. Sci. 36 (2) (2011) 78–87, 10.1016/j.tibs.2010.07.013. [PubMed: 20810284]

[41]. Yamaguchi Y, Ohno J, Sato A, Kido H, Fukushima T, Mesenchymal stem cell spheroids exhibit enhanced in-vitro and in-vivo osteoregenerative potential, BMC. Biotechnol. 14 (1) (2014) 105, 10.1186/s12896-014-0105-9. [PubMed: 25479895]

[42]. Steward AJ, Kelly DJ, Mechanical regulation of mesenchymal stem cell differentiation, J. Anat. 227 (6) (2015) 717–731, 10.1111/joa.12243. [PubMed: 25382217]

[43]. Engler AJ, Griffin MA, Sen S, Bönnemann CG, Sweeney HL, Discher DE, Myotubes differentiate optimally on substrates with tissue-like stiffness, J. Cell Biol. 166 (6) (2004) 877–887, 10.1083/jcb.200405004. [PubMed: 15364962]

[44]. Han S, et al. , The three-dimensional collagen scaffold improves the stemness of rat bone marrow mesenchymal stem cells, J. Genet. Genom. 39 (12) (2012) 633–641, 10.1016/j.jgg.2012.08.006.

[45]. Lo YP, Liu YS, Rimando MG, Ho JHC, Lin K, Lee OK, Three-dimensional spherical spatial boundary conditions differentially regulate osteogenic differentiation of mesenchymal stromal cells, Sci. Rep. 6 (1) (2016) 21253, 10.1038/srep21253. [PubMed: 26884253]

[46]. Song G, Ju Y, Shen X, Luo Q, Shi Y, Qin J, Mechanical stretch promotes proliferation of rat bone marrow mesenchymal stem cells, Colloids. Surf. B Biointerfaces. 58 (2) (2007) 271–277, 10.1016/j.colsurfb.2007.04.001. [PubMed: 17499488]

[47]. Smith PG, Deng L, Fredberg JJ, Maksym GN, Mechanical strain increases cell stiffness through cytoskeletal filament reorganization, Am. J. Phys.Lung Cell. Mole. Physiol. 285 (2) (2003) L456–L463, 10.1152/ajplung.00329.2002.

[48]. Janmey PA, Fletcher DA, Reinhart-King CA, Stiffness sensing by cells, Physiol. Rev. 100 (2) (2020) 695–724, 10.1152/physrev.00013.2019. [PubMed: 31751165]

[49]. Huebsch N, et al. , Harnessing traction-mediated manipulation of the cell/matrix interface to control stem-cell fate, Nat. Mater. 9 (6) (2010) 518–526, 10.1038/nmat2732. [PubMed: 20418863]

[50]. Pek YS, Wan ACA, Ying JY, The effect of matrix stiffness on mesenchymal stem cell differentiation in a 3D thixotropic gel, Biomaterials 31 (3) (2010) 385–391, 10.1016/j.biomaterials.2009.09.057. [PubMed: 19811817]

[51]. Huebsch N, et al. , Harnessing traction-mediated manipulation of the cell/matrix interface to control stem-cell fate, Nat. Mater. 9 (6) (2010) 518–526, 10.1038/nmat2732. [PubMed: 20418863]

[52]. Engler A, Bacakova L, Newman C, Hategan A, Griffin M, Discher D, Substrate compliance versus ligand density in cell on gel responses, Biophys. J. 86 (1) (2004) 617–628, 10.1016/S0006-3495(04)74140-5. [PubMed: 14695306]

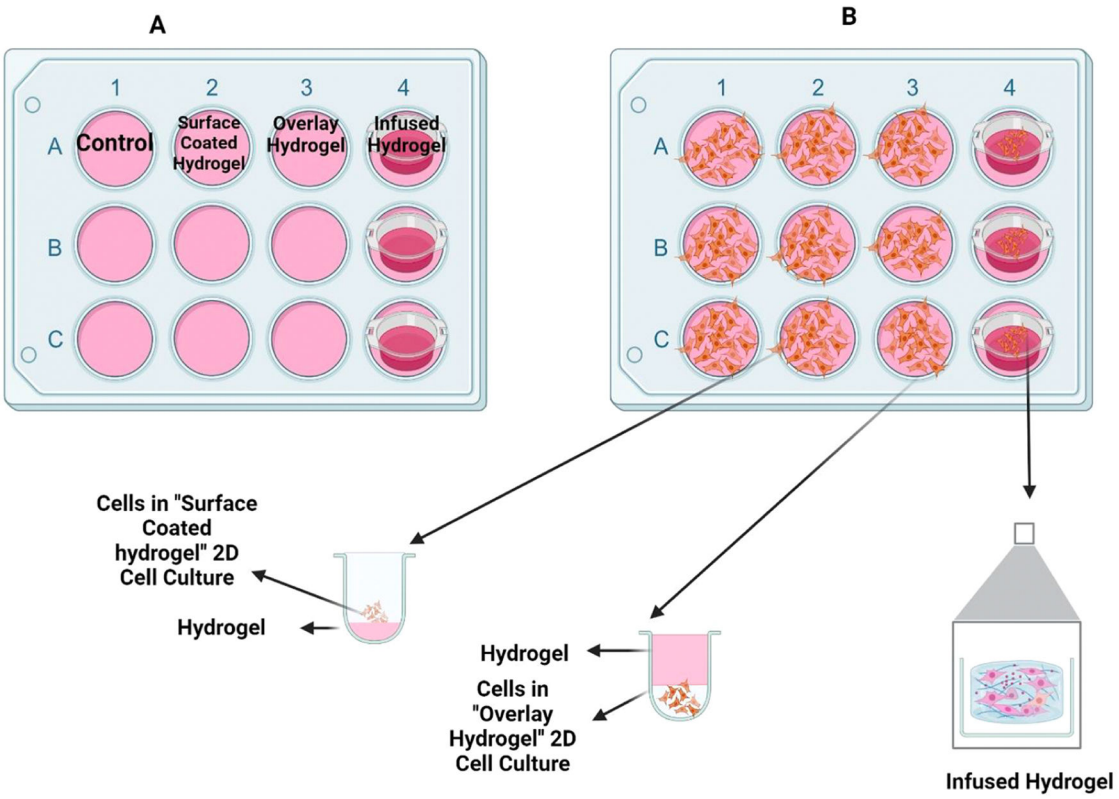

Fig. 1.

Illustration of Fmoc-FF Peptide Hydrogels for MSC cell encapsulation; A) Well preparation with peptide hydrogels; B) MSC in 2D and 3D cultures.

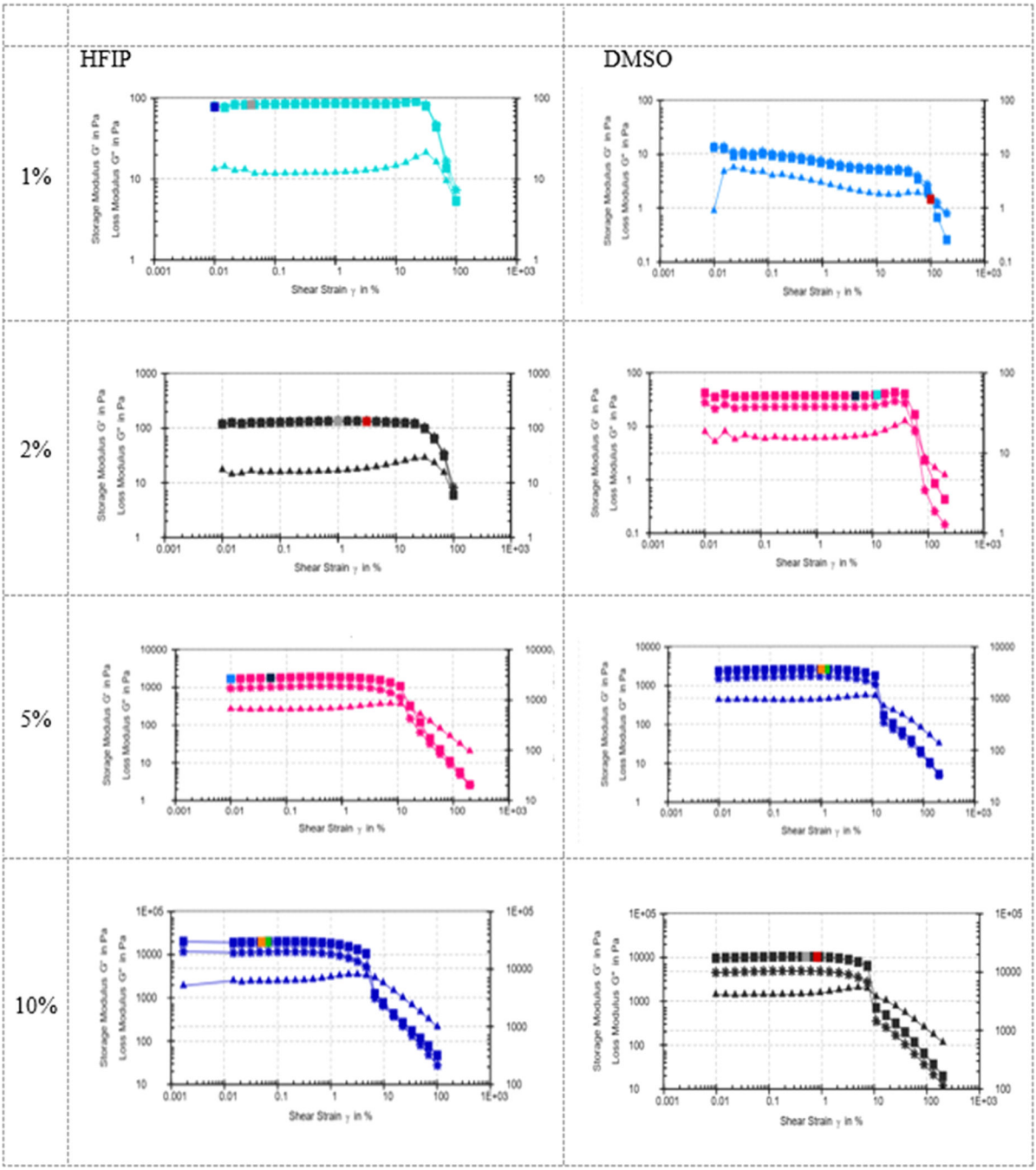

Fig. 2.

Storage Modulus (G': square graph) and Loss modulus (G": triangle graph) of Fmoc-FF in DMSO and in HFP at concentration of 1–10 %.

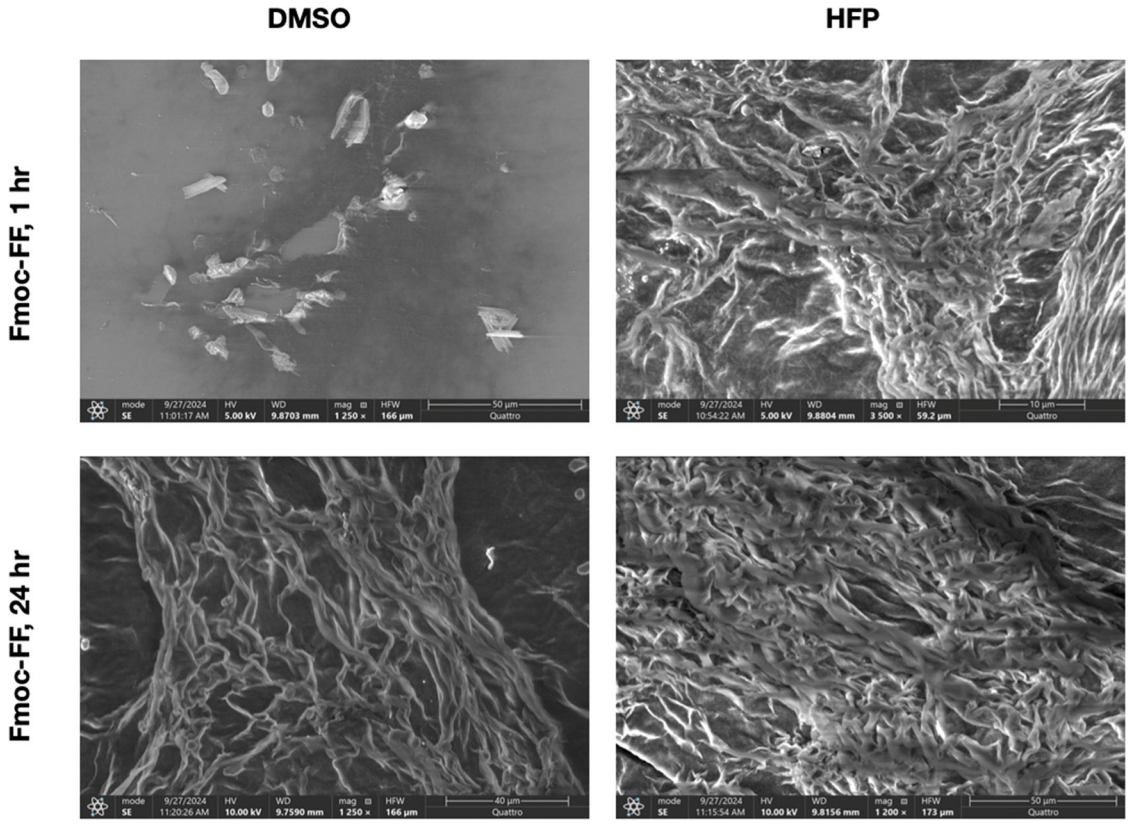

Fig. 3.
SEM image of Fmoc-FF gel in HFP and DMSO after 1 hr and 24 hr.

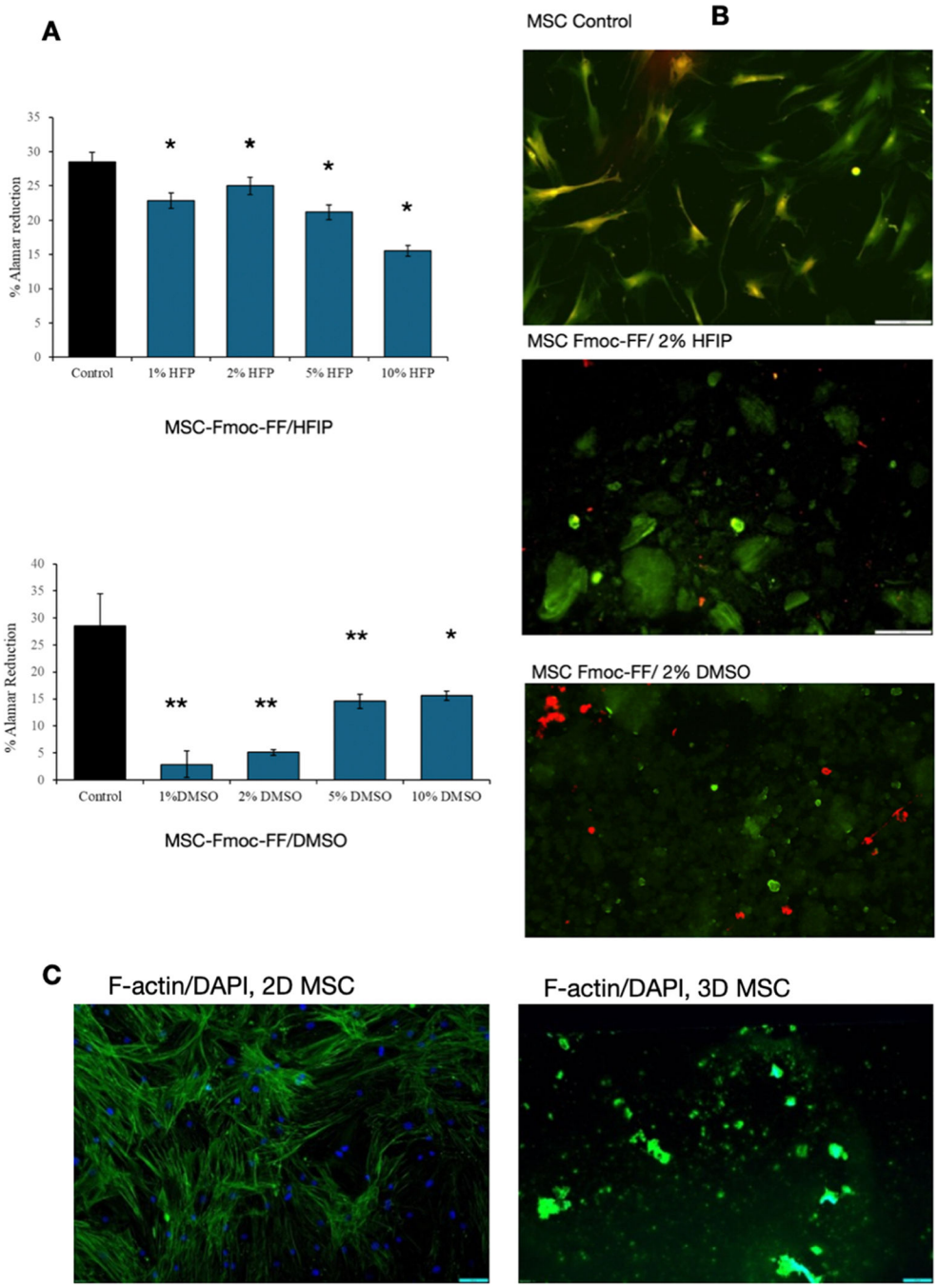

Fig. 4.

Viability assay of MSC seeded in different Fmoc-FF gels with varying percentage and solvent. A) The graph represents the percentage of Alamar Blue reduction, indicating metabolic activity. B) Images of Live/dead assay of MSC infused in GM as control, Fmoc-FF HFIP, and Fmoc-FF DMSO. Live cells are stained green and dead cells are stained red. C) Cytoplasm and nucleus staining of MSC cells. The nucleus is stained blue, and the cytoplasm is stained green.

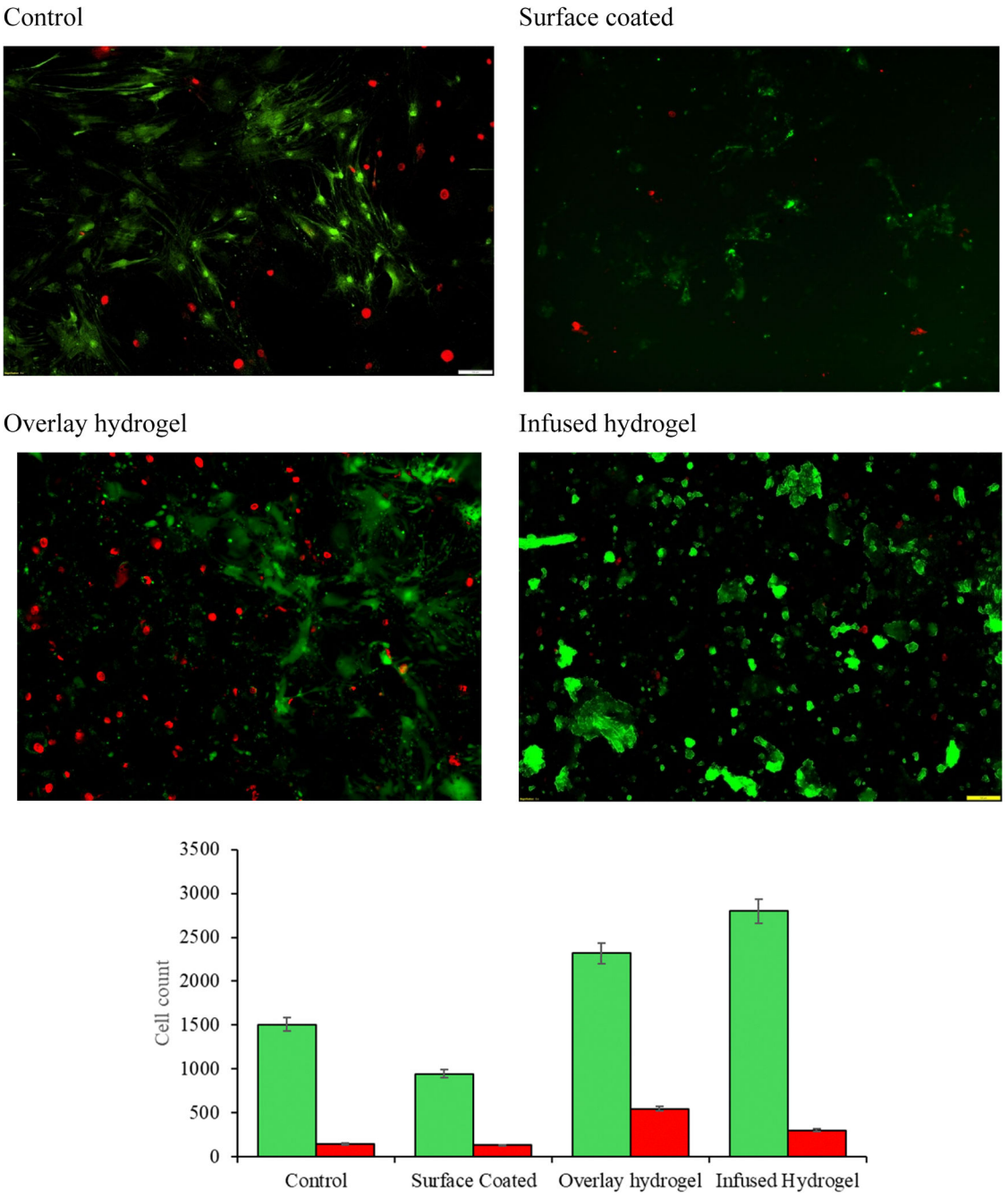

Fig. 5.
Live and dead staining of MSC in OIM seeded in 2D and 3D Fmoc-FF hydrogels.

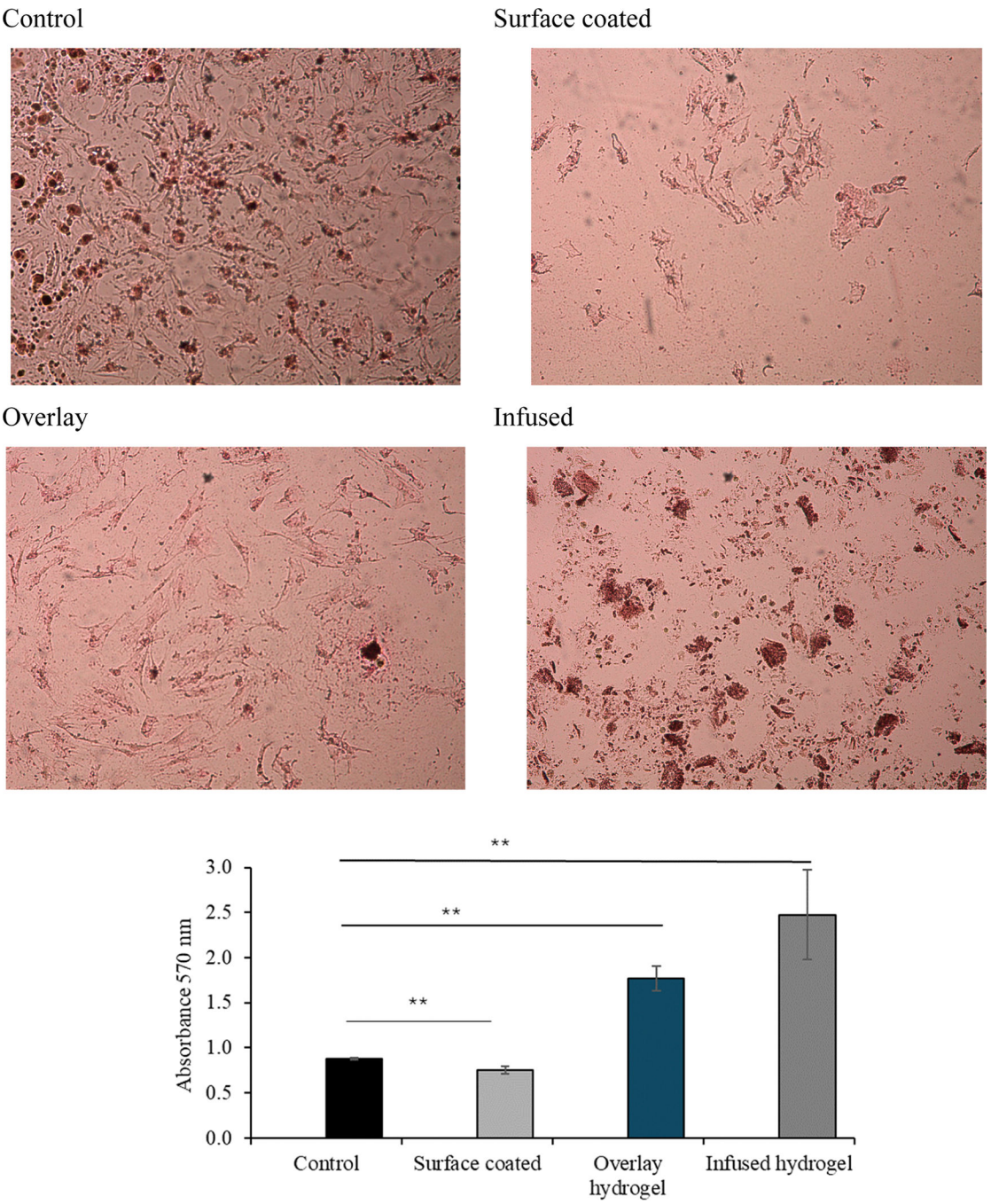

Fig. 6.
Alizarin assay of MSC seeded in Fmoc-FF hydrogels and cultured with OIM.

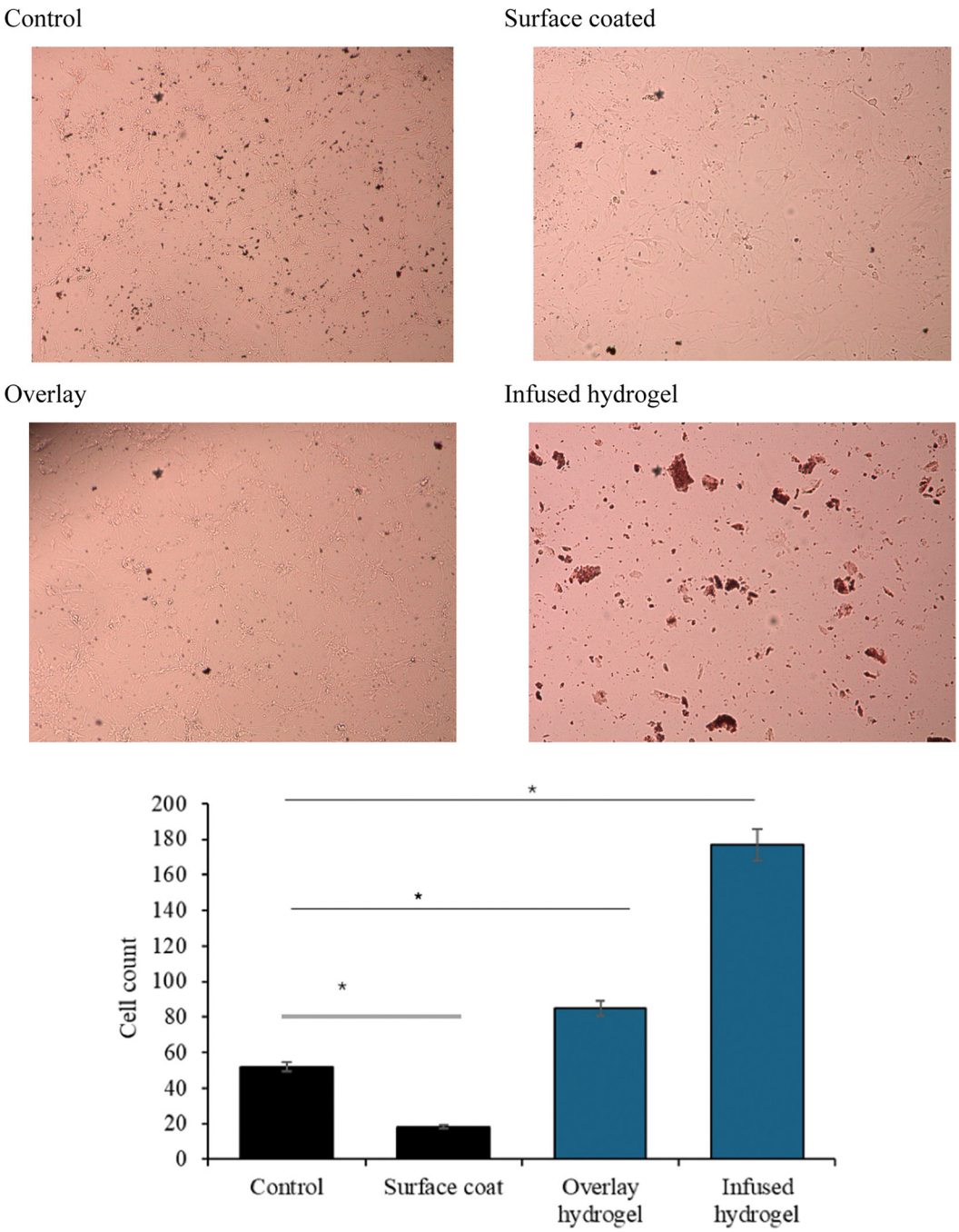

Fig. 7.
ALP assay of MSC seeded in Fmoc-FF hydrogels and cultured with OIM.

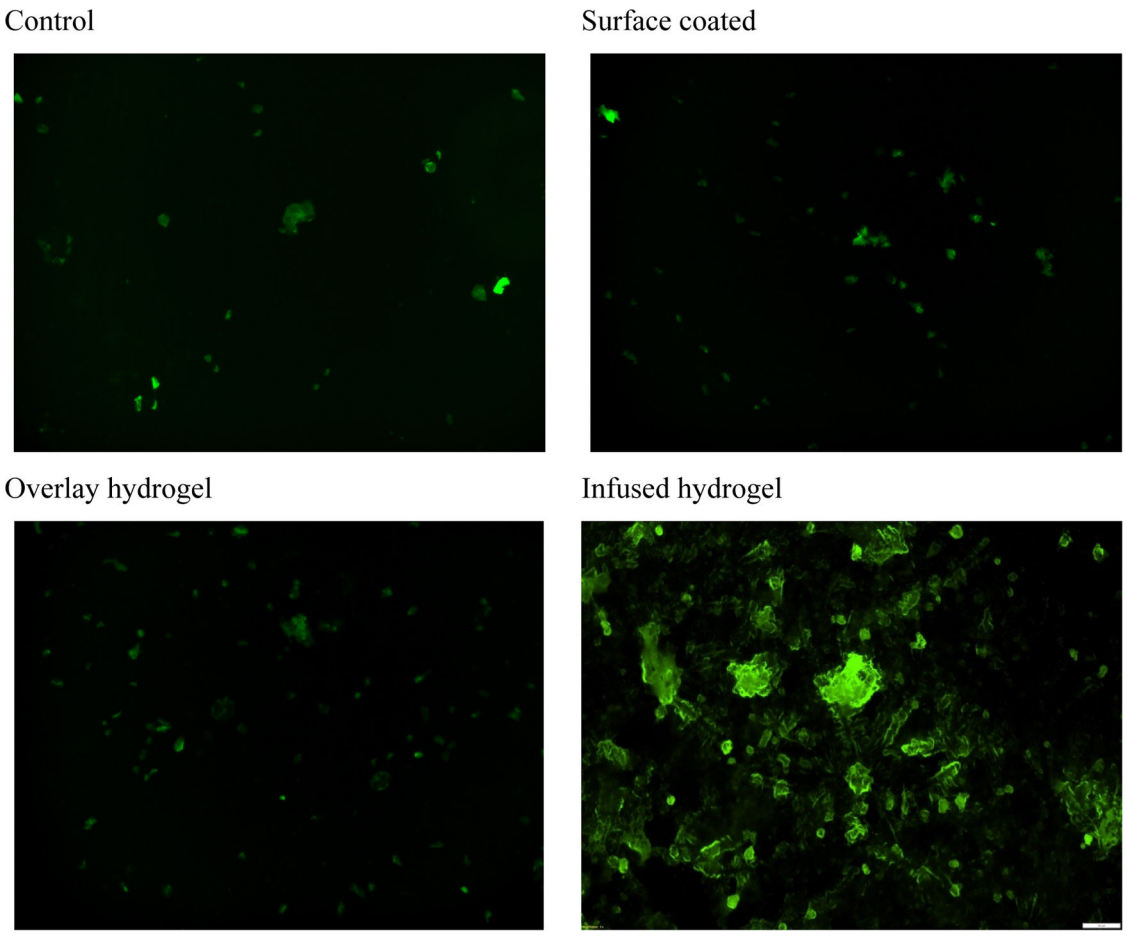

Fig. 8.
Osteocalcin immunostaining of MSC seeded in Fmoc-FF hydrogels.